to crustal thickening under stress from the east or southeast. Salme Dorsa cuts through the ridges of older Sigrun Fossae. Salme Dorsa has quite a recent border scarp and is obviously relatively young. Interlocking nearby ridge belts indicate repeated compressions.

The trough and bulge west of Salme Dorsa is caused by crustal bending due to the ridge belt load or nappe thrust to the west. Tensional grabens along the crest of the bulge indicate crustal extension. The grabens parallel the ridge belt and trough as gentle arcs that open in the direction of Salme Dorsa on the bulge crest. Elastic deformation of the layered crust and adjoining fracturing of the uppermost brittle surface might be reasonable assumptions. The set of narrow grabens on top of the bulge are due to excess tensile stress in the uppermost brittle layer of the lithosphere. The lack of corresponding troughs, bending, or grabens on the eastern side of the ridge belt may indicate that both the load and the thrust from the east have to be taken into account. The volcanic area inside the Salme Dorsa horseshoe have also weakened the crust on that side.

The elastic layer is confined by the temperature above which the upper mantle has negligible strength [1]. The elastic part of the lithosphere is defined by isotherms 450°C and 650°C and this elastic lithosphere is considerably thinner than the low-attenuation seismic lithosphere. The temperature gradients of 15°C/km [2] and 20°C/km [3] and the surface temperature of 470°C suggest that the lower boundary of the elastic lithosphere is about 12 km or 9 km deep, respectively.

The thickness of the elastic layer is estimated using a flexural approach and a two-dimensional model of a semi-infinite broken elastic lithosphere under a linear load [4] with the only acting force, V_0, applied vertically to its end, where the bending moment is zero. The only measurable quantity, x_b, is the distance between the force and the bulge. The equation for the deflection of a plate includes loading of the lithosphere by vertical forces, hydrostatic restoring force, and the position of the bulge. Assuming a basaltic composition for the crust, $r_c = 3000$ kgm^{-3}, $E = 0.6 \times 10^{11}$ Pa and $\upsilon = 0.25$ and using $r_m = 3300$ kgm^{-3}, $g = 8.6$ ms^{-2} and $x_b = 50$ km we find $h \approx 2.9$ km for the elastic thickness of the lithosphere.

Variations in the magnitudes of the vertical or horizontal loads or the bending moment will alter the displacement but will not alter the position of the top of the bulge. Changes in the model, application of a horizontal force or a bending moment, will have more dramatic effects on the distance of the bulge and the lithospheric thickness. If a bending moment is assumed, the thickness of the lithosphere increases due to the increasing effect on plate curvature. The free edge boundary of our model is justified by volcanic activity that has weakened the lithosphere. Both a three-dimensional model and a continuous elastic plate model will reduce the elastic thickness. Allowing a bending moment to act upon the plate end, the elastic thickness of the lithosphere increases by a factor of 2.

The elastically thick lithosphere can support high compressional stresses or fail by faulting rather than buckling. Compressional stress critical to deformation can be estimated [4] to be approximately 0.4 GPa, taking the previous values. The wavelength of the buckling at the critical stress is about 94 km, and is reduced as the stress increases. This value corresponds well to the distance between Salme Dorsa and the bulge, and thus horizontal forces cannot be totally neglected. Recent research has revealed that buckling of the lithosphere can occur at stress levels much less than the elastic strength of the lithosphere [5]. Horizontal forces may have contributed to the buckling but it is difficult to find out which one of the forces has been active for a thickness of the elastic lithosphere of about 3 km. If both forces are allowed [6], the thickness of this layer of the lithosphere is slightly increased to 3.1 km.

Summary: The Salme ridge belt can be interpreted as being the leading edge of a venusian crustal unit that moved against the highland foreland unit. It is indicative of a compressional zone, with a thrust front facing west. The Salme Dorsa ridge belt with adjoining structures is an evident indication of lateral stresses and adjoining crustal movements on Venus. It supports the idea of southeast crustal compression against and over the foreland planitia, which has bent under the load and/or lateral stress, resulting in trough and bulge formation in front of the ridge belt. The origin of the driving force for the movements remains masked. Laima Tessera is located in the direction from which the thrust is thought to apply [7] but there are no appropriate candidates for a rift zone although a thrust from the southeast would be in good agreement with structures of Laima Tessera. The temperature gradient [2] suggests that the lithosphere is approximately 12 km thick, while its elastic layer is approximately 3 km thick based either on the load-induced flexure model or on the compressional buckling model.

References: [1] Kirby S. H. (1983) *Rev. Geophys. Space Phys.*, *21*, 1528–1538. [2] Smrekar S. E. and Solomon S. C. (1992) *Workshop on Mountain Belts on Venus and Earth*, 35–37. [3] Solomon S. C. and Head J. W. (1989) *LPSC XX*, 1032–1033. [4] Turcotte D. L. and Schubert G. (1982) *Geodynamics: Applications of Continuum Physics to Geological Problems*, Wiley, New York, 450 pp. [5] Stephenson R. A. and Cloetingh S. A. P. L. (1991) *Tectonophysics, 188*, 27–37. [6] McAdoo D. A. and Sandwell D. T. (1985) *JGR, 90*, 8563–8569. [7] Raitala J. and Tormanen T. (1990) *Earth Moon Planets, 49*, 57–83.

N93-14365

COMPUTER SIMULATIONS OF COMET- AND ASTEROIDLIKE BODIES PASSING THROUGH THE VENUSIAN ATMOSPHERE—PRELIMINARY RESULTS ON ATMOSPHERIC AND GROUND SHOCK EFFECTS.

D. Roddy[1], D. Hatfield[2], P. Hassig[2], M. Rosenblatt[2], L. Soderblom[1], and E. De Jong[3], [1]U.S. Geological Survey, Flagstaff AZ, USA, [2]California Research & Technology, Chatsworth CA, USA, [3]Jet Propulsion Laboratory, Pasadena CA, USA.

We have completed computer simulations that model shock effects in the venusian atmosphere caused during the passage of two cometlike bodies 100 m and 1000 m in diameter and an asteroidlike body 10 km in diameter. Our objective is to examine hypervelocity-generated shock effects in the venusian atmosphere for bodies of different types and sizes in order to understand (1) their deceleration and depth of penetration through the atmosphere and (2) the onset of possible ground-surface shock effects such as splotches, craters, and ejecta formations. The three bodies were chosen to include both a range of general conditions applicable to Venus as well as three specific cases of current interest.

These calculations use a new multiphase computer code (DICE–MAZ) designed by California Research & Technology for shock-dynamics simulations in complex environments. The code has been tested and calibrated in large-scale explosion, cratering, and ejecta research. It treats a wide range of different multiphase conditions, including material types (vapor, melt, solid), particle-size distributions, and shock-induced dynamic changes in velocities, pressures, temperatures (internal energies), densities, and other related parameters, all of which were recorded in our calculations. DICE–MAZ is especially useful in our Venus study because of the advance capability in multiphase adaptive zoning and because of the color coding associated with displaying the complex variations in

DICE-MAZ M201 (2-D VENUS, 100 M, Link-2) R07 M201PL1
CYCLE= 2724, TIME= 10.00 S
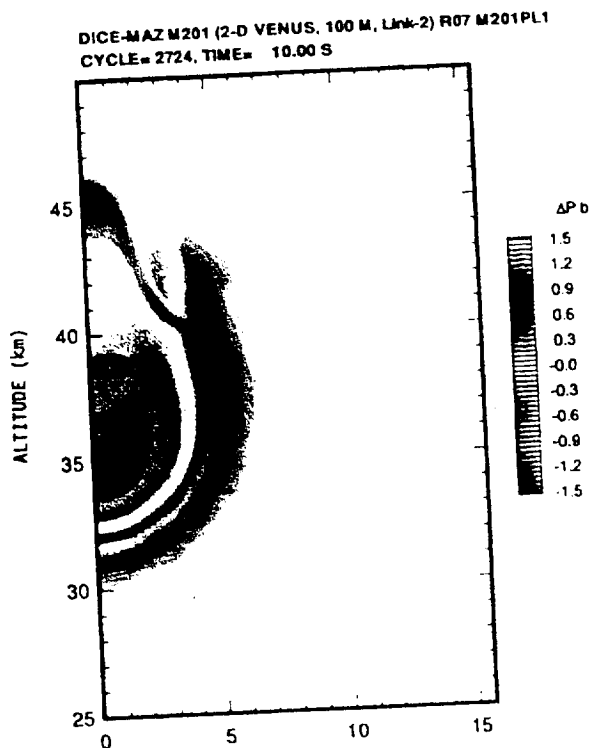
Fig. 1. Numerical simulation of bow shock-wave pressure field (ΔPb) surrounding the highly dispersed 100-m-diameter body now composed of vapor, melt (?), and original fragments at about 32-km altitude. The highest pressure in the bow shock wave is about 1.5 bar and is too weak to effect the venusian surface.

dynamic changes in parameters for the shocked bodies and surrounding atmosphere.

This preliminary study modeled the venusian atmosphere following [1], but without winds. An initial velocity of 20 km/s with a vertical trajectory was assumed for all cases. The 100-m and 1000-m bodies had a mean density of 1.0 g/cm³ (cometlike) and the 10-km body had a mean density of 2.5 g/cm³ (asteroidlike). For the 100-m and 1000-m cometlike bodies, the basic calculations were started at an altitude of 80 km; the complete numerical simulations were started at 45 km altitude, where deceleration of the 100-m body became significant. At altitude, on the order of 45 km, shock pressures in excess of 5 kbar were calculated at the leading edge of these bodies. We believe that these large differential body pressures could catastrophically break up low-strength, low-density bodies in the size range chosen. Therefore, we elected to model these two cases as fragmented for the remainder of their descent below 45 km into Venus' atmosphere. Fragmentation distributions of equal total mass per decade size bins ranging between 0.01 and 1000 cm were used. Consequently, the simulations represent only one plausible set of a wide range of possible body strengths, fragmentation histories, and entry conditions that remain to be explored. The 10-km body was assumed to not fragment under our initial conditions and was modeled as a rigid, nondeformable sphere; this choice was made mainly to permit direct comparisons with a similar set of calculations of asteroid impacts on the Earth in which the atmosphere is not dense enough to induce fragmentation for a body this size [2]. A fragmenting body 10 km in size should be calculated for direct comparisons with the other two bodies modeled here for Venus, but this was beyond the scope of our preliminary study. Oblique

trajectories are also important and the three-dimensional capability of the DICE–MAZ code should be used in later studies.

The 100-m-diameter fragmented body decelerated rapidly between 45 km and about 32 km altitude and the majority of its fragments were converted to vapor due to shock heating. The vapor and fragments experienced extensive outward separation due to flow along the bow shock wave generated in the atmosphere. The body took about 10 s to travel from 45 km down to about 32 km altitude with continuous deceleration and dispersion as vapor, melt (depending on materials present), and original fragments. These materials expanded to about 5 km across in a low-density band immediately behind the downward moving bow-shock wave. At about 32 km altitude, the dispersed vapor (~75%) was expanding in all directions and the remaining original fragments (~25%), including any melt, were in free fall to the surface. At about 32 km altitude, the pressure in the bow shock wave had decayed to about 1 bar and would produce no effect on the venusian surface.

The 1000-m-diameter fragmented body traveled downward in an increasingly dispersed configuration from 45 km altitude to the venusian surface in about 4.5 s, decelerating less rapidly than the 100-m body. As in the case of the 100-m body, the 1000-m body decelerated and dispersed as vapor, melt (depending on materials present), and original fragments. These materials spread into in a narrow band behind the bow-shock wave as the entire system penetrated downward in the atmosphere and expanded finally to over 10 km across near the ground. In this case, the 1000-m body had sufficient size and energetics to create a strong bow shock that reached the venusian surface with pressures of about 2.0 kbar at ground zero and decayed to 100 bar at 15 km ground range. The bow shock was followed immediately by a band of low-density, dispersed vapor (~25%) and original fragments (~75%), including melt (?), moving down and radially outward with peak horizontal velocities of about 0.5 km/s in the atmosphere at ranges of 10 km from ground zero (about 10 s). Of course, no impact-cratering effects occurred because the density and velocity of vapor and

DICE-MAZ M204: 2-D VENUS, D = 1000 m
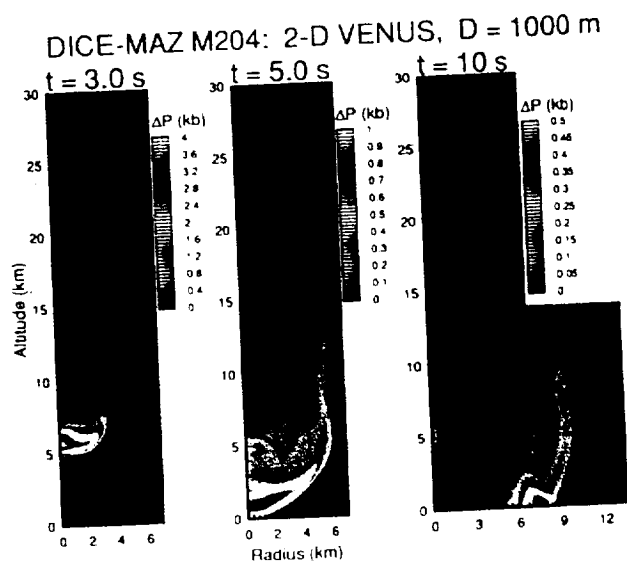
Fig. 2. Numerical simulations of bow shock wave pressure fields (ΔPkb) surrounding the dispersed 1000-m-diameter body that consists of vapor, melt (?), and original fragments. At 4.5 s, the leading edge of the bow shock has reached the venusian surface with a peak pressure of about 2.0 kbar at ground zero and decays to 100 bar at 15 km range; at 10 s, peak horizontal velocities in the atmosphere are about 0.5 km/s at 10 km range.

fragments were too low to induce a ground-shock condition sufficient for cratering. However, we do suggest that this body developed bow-shock peak overpressures and shock-initiated winds in the atmosphere near the ground sufficient to cause incipient disturbances on the venusian surface, depending on rheologic states of the target materials.

The 10 km-diameter body traveled from 45 km altitude down to the surface in 2 s with less than 2% deceleration and would have caused major atmospheric, impact-cratering, and ejecta effects. We estimate that the final crater would have been 150 to 200 km across but only a few kilometers deep, which we infer would be due in part to the high temperature, low strength, rapid relaxation rate of the target rock. This large body generated an enormous bow-shock wave with pressures in excess of 600 kbar that reached the ground surface and swept outward at over 10 km/s. It also evacuated a region over 40 km in diameter along the trajectory of the body in the atmosphere. This hot (~20,000–200,000 K), low-density region continued to expand and remained open for over several minutes after impact with substantial amounts of high-angle ejecta traveling through it to high altitudes. The effects of the 10-km body in Venus' environment are still under analysis, but several of the major aspects appear similar to the asteroid-impact results calculated for the Earth. The energetics of such large events tend to initially overwhelm both atmospheres.

In summary, our numerical simulations indicate that for weak, cometlike objects impacting into Venus' atmosphere at 20 km/s, a 100-m-diameter body completely disintegrates at high altitude and produces no ground surface effects. A 1000-m-diameter body also disintegrates but produces a strong bow-shock wave immediately followed by a dispersed band of vapor, melt (?), and fragments that reach the ground to produce strong shock pressures and radial winds in the near-ground atmosphere. We suggest that these conditions could induce incipient surface disruption and produce subtle surface features, depending on the rheologic states of the target materials. We suspect that the dark and light splotches that are several tens of kilometers in diameter seen in the Magellan SAR images [3–8], and believed to be impact induced, could have been generated by cometlike bodies a few kilometers in diameter. The bodies could be somewhat smaller if the splotches were produced by stronger asteroidlike bodies that fragmented lower in the atmosphere; these cases remain to be explored.

References: [1] Seiff A. (1983) In *Venus*, 1045–1048, Univ. of Arizona, Tucson. [2] Roddy D. J. et al. (1987) *Int. J. Impact Engng.*, 525–541. [3] Arvidson R. E. et al. (1991) *Science*, 270–275. [4] Phillips R. J. et al. (1991) *Science*, 288–297. [5] Zahnle K. J. (1991) *Eos*, 44, 289. [6] Zahnle K. J. (1992) *LPSC XXIII*, 1565. [7] Soderblom L. A. et al. (1992) *LPSC XXIII*, 1329–1330. [8] Schaber G. G. et al., in press.

N93-14366

THE EFFECTS OF VENUS' THERMAL STRUCTURE ON BUOYANT MAGMA ASCENT.

S. E. H. Sakimoto and M. T. Zuber, Department of Earth and Planetary Sciences, The Johns Hopkins University, Baltimore MD 21228, USA.

The recent Magellan images have revealed a broad spatial distribution of surface volcanism on Venus [1]. Previous work in modeling the ascent of magma on both Venus and Earth [2–5] has indicated that the planetary thermal structure significantly influences the magmatic cooling rates and thus the amount of magma that can be transported to the surface before solidification. In order to understand which aspects of the thermal structure have the greatest

influence on the cooling of ascending magma, we have constructed magma cooling curves for both plutonic and crack buoyant ascent mechanisms, and evaluated the curves for variations in the planetary mantle temperature, thermal gradient curvature with depth, surface temperature gradient, and surface temperature. The planetary thermal structure is modeled as

$$\frac{T}{T_0} = 1 - \tau\left(1 - \frac{Z}{Z_0}\right)^n \qquad (1)$$

where T is the temperature, T_0 is the source depth temperature, $\tau = 1 - (T_s/T_0)$ where T_s is the planetary surface temperature, Z is the depth, Z_0 is the source depth, and n is a constant that controls thermal gradient curvature with depth. Equation (1) is used both for mathematical convenience and flexibility, as well as its fit to the thermal gradients predicted by the cooling half-space models [6]. We assume a constant velocity buoyant ascent, body-averaged magma temperatures and properties, an initially crystal-free magma, and the same liquidus and solidus for both Venus and Earth.

The cooling model for the plutonic ascent has been described in detail in earlier publications [2–5], and is a low Reynolds number, high Peclet number problem of heat transfer through a thin thermal boundary layer around a sphere. The resulting plutonic cooling curves, which are dominated by the convective cooling terms and strongly influenced by the planetary thermal structure, are then expressed mathematically by

$$\frac{T}{T_0} = \frac{J}{J+\gamma}\left(1 - e^{-(J+\gamma)t}\right) + e^{-(J+\gamma)t} + \left(\frac{J}{J+\gamma}\right)\left(\frac{\tau}{[(J+\gamma t_0)]^n}\right)$$

$$\left[e^{-(J+\gamma)t}(-1)^n n! - \sum_{p=0}^{n}\frac{(-1)^p n!\left[(J+\gamma)t\right]^{n-p}}{(n-p)!}\right] \qquad (2)$$

Earth
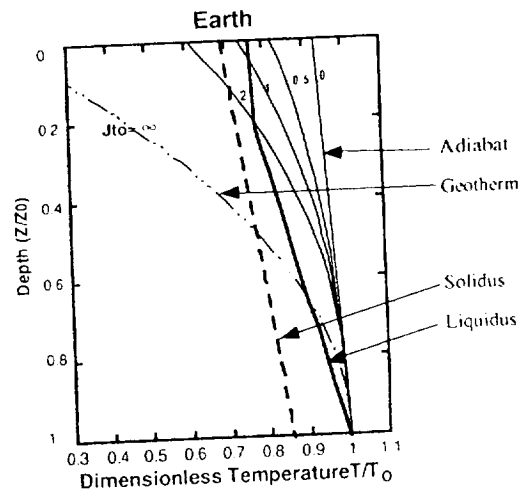
Fig. 1. Example of a typical cooling curve plot for pluton ascent. The curves are plotted for a given thermal structure and/or planet, and are contoured with their associated dimensionless ascent (Jt_0) values. In order for the magma to reach the surface unsolidified, the cooling curve must not cross the solidus. This plot is for a dry olivine tholeiite. The liquidus and solidus are obtained from [11]. Thermal structure parameters: n = 2; dT/dZ = 1.0 (dT/dZ of Earth); Z_0 = 1.0 (Z_0 of Earth).